



## RiArsB and RiMT-11: Two novel genes induced by arsenate in arbuscular mycorrhiza

Ignacio E. Maldonado-Mendoza<sup>a, \*</sup>, Maria J. Harrison<sup>b</sup>

<sup>a</sup> Instituto Politécnico Nacional, Centro Interdisciplinario de Investigación para el Desarrollo Integral Regional (CIIDIR)-IPN Unidad Sinaloa, Departamento de Biotecnología Agrícola, Blvd. Juan de Dios Bátiz Paredes No. 250, AP280, Guasave, Sinaloa CP81101, Mexico

<sup>b</sup> Boyce Thompson Institute, 533 Tower Road, Ithaca, NY 14853-1801, USA

### ARTICLE INFO

#### Article history:

Received 31 May 2017

Received in revised form

9 October 2017

Accepted 9 November 2017

Available online 28 November 2017

Corresponding Editor: Alga Zuccaro

#### Keywords:

Arbuscular mycorrhizal fungi

Arsenic detoxification

Arsenite efflux pump

Methyl transferases

*Rhizophagus irregularis*

### ABSTRACT

Plants associated with arbuscular mycorrhizal fungi (AMF) increase their tolerance to arsenic-polluted soils. This study aims to investigate the genes involved in the AMF molecular response to arsenic pollution. Genes encoding proteins involved in arsenic metabolism were identified and their expression assessed by PCR or RT-qPCR. The As-inducible gene *GiArsA* (*R. irregularis* ABC ATPase component of the *ArsAB* arsenite efflux pump) and two new genes, an arsenate/arsenite permease component of *ArsAB* (*RiArsB*) and a methyltransferase type 11 (*RiMT-11*) were induced when arsenate was added to two-compartment *in vitro* monoxenic cultures of *R. irregularis*-transformed carrot roots. *RiArsB* and *RiMT-11* expression in extraradical hyphae in response to arsenate displayed maximum induction 4–6 h after addition of 350  $\mu$ M arsenate. Their expression was also detected in colonized root tissues grown in pots, or in the root-fungus compartment of two-compartment *in vitro* systems. We used a *Medicago truncatula* double mutant (*mtpt4/mtpt8*) to demonstrate that *RiMT-11* and *RiArsB* transcripts accumulate in response to the addition of arsenate but not in response to phosphate. These results suggest that these genes respond to arsenate addition regardless of non-functional Pi symbiotic transport, and that *RiMT-11* may be involved in arsenate detoxification by methylation in AMF-colonized tissues.

© 2017 British Mycological Society. Published by Elsevier Ltd. All rights reserved.

### 1. Introduction

Arbuscular mycorrhizal fungi (AMF) of the phylum Glomeromycota form obligate endosymbiotic associations with the majority of vascular flowering plants, in all types of soil (Smith and Read, 2008; Lanfranco and Young, 2012). AMF obtain carbon from the plant, which allows them to complete their life cycle, while providing benefits to the plant such as improved mineral nutrition (Smith and Smith, 2011) and increased plant tolerance to heavy metal pollution (Hildebrandt et al., 2007).

AMF naturally associate with plants in arsenic (As) contaminated soils (Smith et al., 2010). Indeed, AMF are reported to improve plant tolerance to As in species such as maize (Bai et al., 2008), tomato (Liu et al., 2005), plantain (Orłowska et al., 2012), Chinese fern (Leung et al., 2010), white clover and ryegrass (Dong et al., 2008). This AMF-mediated increase in tolerance to As in plants could be due to different mechanisms, such as the improvement of

plant P nutrition, or growth that causes an indirect “dilution effect” on As in plant tissues (Chen et al., 2007; Xia et al., 2007; Xu et al., 2008). AMF are also capable of modulating As uptake by the plant. For instance, González-Chávez et al. (2002) observed a reduced influx of arsenate [As(V)] into *Holcus lanatus* excised roots, while Christophersen et al. (2009) reported that As(V) uptake in barley is reduced by arbuscular mycorrhizal (AM) colonization via down-regulation of the plant high-affinity phosphate transporters that regulate As(V) uptake.

AMF may also contribute to an increased As tolerance in plants via an As exclusion mechanism. This has been suggested in *Rhizophagus irregularis*, which demonstrates As(V) uptake via a fungal high-affinity phosphate transporter (*GiPT*); As(V) is subsequently reduced to arsenite [As(III)] and pumped out of fungal cells by an arsenite efflux pump (González-Chávez et al., 2011). This is possibly mediated by a putative *ArsAB* arsenite efflux pump, which may be similar to bacterial efflux pumps (Dey and Rosen, 1995). In *Escherichia coli* *ArsA* corresponds to the catalytic component of the pump (Rosen et al., 1988), and *ArsB* is an intrinsic membrane protein (San Francisco et al., 1989; Wu et al., 1992), that anchors the *ArsA* protein and works as an anion channel (Tisa and Rosen, 1990).

\* Corresponding author.

E-mail address: [imaldona@ipn.mx](mailto:imaldona@ipn.mx) (I.E. Maldonado-Mendoza).

The ABC ATPase component (*GiArsA*) in AMF is known to be induced as rapidly as 3 h after As exposure in external hyphae, and after the induction of *GiPT* transcript levels (González-Chávez et al., 2011) supporting this possible exclusion mechanism. The arsenite permease component of the efflux pump (*ArsB*) has not been described yet. More recently, analysis by microspectroscopic X-ray fluorescence ( $\mu$ -XRF) and microspectroscopic X-ray absorption near edge structure ( $\mu$ -XANES) has confirmed that As(V) is absorbed into the external hyphae of AMF after 1 h, and reduced to As(III) within 6 h. Arsenic is observed during this period as different compounds, the most dominant species being the As(III)–Fe(II) carbonate form followed by less abundant forms such as As(V)–Fe(III) hydroxide and As(III)–sulfur compounds. No detectable As concentrations could be found in the external mycelium after 24 or 72 h, confirming that any previously absorbed As had been pumped out from the hyphae (González-Chávez et al., 2014).

AMF can also affect As(V) toxicity by decreasing oxidative stress (Yu et al., 2009; Garg and Singla, 2012), and by causing a differential distribution of As species in plants (Yu et al., 2009; Chen et al., 2012). Zhang et al. (2015b) demonstrated that AM fungi can enhance As tolerance in *Medicago truncatula* by improving plant P nutrition and influencing As accumulation and speciation. The authors found that mycorrhizal colonization increased shoot and root P concentrations and significantly reduced As concentrations. The percentage of As(III) in the total As pool increased significantly in mycorrhizal plants, especially under low P supply. Furthermore, the authors provided clear evidence, in the *M. truncatula* non-mycorrhizal mutant TR25:3-1, of the role that AMF play in plant tolerance to As under natural conditions, as well as its role in methylation of inorganic As into less toxic organic dimethylarsinic acid (DMA). DMA was found only in the shoots of mycorrhizal wild type plants, and not in the non-mycorrhizal mutant. DMA has been suggested to be actively transported from roots to shoots in rice plants (Jia et al., 2012) which may help explain why DMA is only found in the *M. truncatula* shoots of mycorrhizal plants.

The involvement of AMF in increasing As(III) in plants and in methylating inorganic As into DMA (Zhang et al., 2015a,b) is in agreement with the findings regarding As(III) formation and its exclusion in *Glomus intraradices* (González-Chávez et al., 2011, 2014), as well as opens the possibility for the presence of a gene product that is capable of methylating As(III) forms.

The possible mechanisms involved in the transport and detoxification of As by AMF are starting to be deciphered, although much remains to be understood. The goal of the present work was to investigate the mechanisms of As transport and detoxification in AMF, using the available *R. irregularis* transcriptome and genome databases. This allowed us to identify putative gene homologs for different components of the arsenic transport mechanism. Based on our study of transcript level accumulation in response to arsenate addition, we present two novel genes, *RiArsB* a putative arsenate/arsenite permease which could be part of the *ArsAB* arsenite efflux pump and *RiMT-11*, a putative methylase which could methylate As to create less toxic forms and which may be involved in As detoxification in arbuscular mycorrhiza.

## 2. Materials and methods

### 2.1. *M. truncatula* mutants

*M. truncatula tricycla* (R108) was used for all experiments. The *mtpt4-5 mtpt8-1* double mutant plants are in the R108 background and the mutant genes are Tnt1 insertion alleles. The *M. truncatula* Tnt1 lines used in this study were TNK22 for *pt4-5*, and NF5213 for *pt8-1*. The double mutant was generated by crossing the respective single mutants, *pt8-1* and *pt-4-5* (Breuillin-Sessoms et al., 2015).

### 2.2. *R. irregularis* colonization of *M. truncatula*

The *M. truncatula* ssp. *truncatula* ecotype Jemalong (A17), colonized by *R. irregularis* [(Biaszk., Wubet, Renker, and Buscot) C. Walker and A. Schüßler comb. nov., (Stockinger et al., 2009)], previously known as *G. intraradices* DAOM197198, was used to confirm the expression of genes in wild type root tissues. Plants were grown in growth rooms under a 16 h light (25 °C)/8 h dark (22 °C) regime. *R. irregularis* was maintained in cultured carrot roots (*Daucus carota*) on two-compartment plates (St-Arnaud et al., 1996), and spores were prepared from the fungal side of the plates according to a modification of Doner and Bécard (1991) protocol. The solid medium was liquefied in an equal volume of 10 mM sodium citrate (using a blender on high setting for 5–10 s). Subsequently, the fungal material was sieved using 50- $\mu$ m nylon meshes. The separated spores were then suspended in 10 mL of distilled water, counted under a stereoscope, and adjusted to 400 spores/mL in water. Two-day-old *M. truncatula* seedlings were planted into 0.2 L cones containing a 1:1 mixture of gravel:sand with a layer of fine sand and 1000 *R. irregularis* spores (2.5 mL of spore suspension) placed by pipetting on top of the sand layer, covered with a 6 cm layer of gravel:sand mixture and fertilized twice weekly with half-strength Hoagland's solution containing 20  $\mu$ M potassium phosphate. Plants were then harvested four weeks after inoculation. The average colonized root length was above 40 %, as estimated by the modified gridline intersection method (McGonigle et al., 1990).

Double mutant plants were grown in large Petri dishes (150 mm  $\times$  35 mm) containing sterile sand and 40 mL liquid M medium (containing 35  $\mu$ M phosphate). *M. truncatula* seeds were sterilized and germinated in sterile conditions on 35-mm-deep Petri plates by adding water, according to Floss et al. (2013). Seedlings (18–24 h old) were installed in the Petri plates through a hole in the cover sealed with sterile lanolin, and the seedling root system was placed on top of an agar plug containing *R. irregularis* hyphae and spores from a two-compartment system. This allowed the root system to be kept sterile, while maintaining the growing plantlets in a growth chamber inside plastic domes to avoid dehydration. Plants were kept for 10 weeks under a 16 h light (25 °C)/8 h dark (22 °C) regime and were fertilized through a hole made in the plate lid that was covered with sterile tape. Watering frequency was once every two weeks with new M liquid medium (20 mL per application) in low nitrogen (1.22 mM Ca (NO<sub>3</sub>)<sub>2</sub>·4H<sub>2</sub>O + 0.79 mM KNO<sub>3</sub>) without any phosphate (for phosphate-deprived growth). Percentage of colonization at week 10 was 89.52 %  $\pm$  10.37 in R108 wild type plants and 26.18 %  $\pm$  13.28 in the *mtpt4/mtpt8* double mutants. Non-colonized control plants did not exhibit any AMF structure. The low N fertilization regime allowed observing the *pt4/pt8* double mutant phenotype as wild type (Breuillin-Sessoms et al., 2015). For arsenate treatment, 25 mL of 350  $\mu$ M sodium arsenate dissolved in water were administered at week 10, whereas the control plates only received water. Roots were harvested after 4 h and 24 h.

### 2.3. Two-compartment plate system

Two-compartment plates containing the DC1 line of transformed carrot roots colonized with *R. irregularis* (Bécard and Fortin, 1988) were used according to Maldonado-Mendoza et al. (2001), in which the fungal compartment was prepared with liquid M medium instead of solid agar M medium. Plates were used as described in González-Chávez et al. (2011). Briefly, the plates were cultured until phosphate was depleted, with phosphate levels in the fungal compartment >1  $\mu$ M Pi. New liquid medium was then added to the fungal compartment, with different arsenate or phosphate concentrations. Experiments with different concentrations of arsenate,

such as (NaH<sub>2</sub>AsO<sub>4</sub>·7H<sub>2</sub>O)/phosphate (NaH<sub>2</sub>PO<sub>4</sub>), required three plates sampled per time point. For time–dose–response experiments, the fungal tissue was obtained from a single plate, and three plates were analyzed. For each plate and time point, a liquid medium aliquot (0.3 mL) was withdrawn to measure the arsenate/phosphate concentrations. The experimental use of two-compartment systems can result in a difference in biomass growth between each experimental unit, leading to different uptake rates of the metalloid added to each system. In order to address this problem, each experiment was conducted in triplicate, in independent experimental units. Each individual experiment was conducted at least twice. The liquid medium and fungal tissue were sampled at different time points, in order to measure the amount of phosphate/arsenate remaining in the medium. Fungal tissue was then processed to obtain total RNA.

#### 2.4. Phosphorus and arsenic determination

The phosphate content of the liquid medium was measured using the phosphomolybdate colorimetric reaction (Ames, 1966) before and after the addition of new medium, and at the time of harvest. Arsenate was calculated based on a standard curve using sodium arsenate (NaH<sub>2</sub>AsO<sub>4</sub>·7H<sub>2</sub>O) instead of sodium phosphate (NaH<sub>2</sub>PO<sub>4</sub>), in order to calculate phosphate levels in the liquid medium. Plates were used only if the phosphate concentration in the medium was below 1 μM. Throughout the experiments, plates contained 5–15 % less arsenate after 24 h of arsenate addition (350 μM) than at time zero, as previously observed (~12 %; González-Chávez et al., 2011).

#### 2.5. Primer design

Primer design was performed using the Primer 3 Plus software (<http://www.primer3plus.com/cgi-bin/dev/primer3plus.cgi>) for all nine genes discovered by data mining. Primers for quantitative RT-PCR were designed to amplify 90–200 bp regions (Table 1), with annealing temperatures close to 60 °C.

#### 2.6. RNA extraction and quantitative RT-PCR

Total RNA from fungal tissue was obtained by freezing the dry-blotted mycelia in liquid nitrogen. The tissue was then macerated using a mortar and pestle, treated using TRIzol<sup>®</sup> Reagent (Thermo Fisher Scientific, Cat. No. 15596-026; Waltham, MA, USA), and ground until it was liquefied. The suspension was collected in 2-mL tubes and RNA was extracted according to the manufacturer's instructions. Total RNA was treated with RNase-free Turbo<sup>™</sup> DNase I (Thermo Fisher Scientific, Cat. No. AM2238), followed by a chloroform purification step. First-strand cDNAs were synthesized from 500 ng DNase-treated RNA using SuperScript III reverse

transcriptase (Thermo Fisher Scientific, Cat. No. 18080044) in a 20 μL reaction. For quantitative real-time RT-PCR, transcripts were amplified from 2.5 μL of 5× diluted cDNA (100 ng) in a 10 μL reaction using gene-specific primers with the SYBR<sup>®</sup> Green PCR Mastermix, using an ABI PRISM 7900 HT Sequence Detection System. The PCR conditions were set for 94 °C at 5 min, followed by 40 cycles of 94 °C (30 s), 60 °C (30 s), and 72 °C (30 s); a dissociation curve was generated at the end. The generated threshold cycle (CT) was used to calculate the transcript abundance relative to the housekeeping gene *R. irregularis* α-tubulin, using the comparative threshold cycle method  $2^{-\Delta\Delta Ct}$  as reported in Cervantes-Gómez et al. (2015).

#### 2.7. Protein analysis software

Four different software programs were used to predict transmembrane helix domains for the RiArsB protein, one of which predicted nine transmembrane helices (HMMTOP, <http://www.enzim.hu/hmmtop/>) while the other three predicted ten helices (TMpred, <http://www.expasy.org/tools/>; PredictProtein, <http://ppopen.informatik.tu-muenchen.de/>; and Protter [Phobius], <http://wlab.ethz.ch/protter/start/>). Different software was used to predict RiArsB and RiMT-11 protein localization (PredictProtein), physiological parameters (ProtParam; <http://www.expasy.org/tools/>), putative motifs (Protter), and conserved domains (GenBank; <https://www.ncbi.nlm.nih.gov/genbank/>).

### 3. Results

#### 3.1. Expression of putative arsenic-related genes

Seven genes putatively involved in As transport or detoxification were identified in this study via data mining of the *R. irregularis* genome (<http://genome.jgi.doe.gov/Gloin1/Gloin1.home.html>) and transcriptome (Mycor Web, <http://mycor.nancy.inra.fr/IMGC/GlomusGenome/index3.html>). These genes were selected based on nucleotide, protein and functional (regulatory protein domain) homology to orthologous genes from prokaryotic (*E. coli*) or eukaryotic (*Saccharomyces cerevisiae* and *Neurospora crassa*) organisms, in which As transport and detoxification systems have already been characterized. Six out of the seven investigated genes displayed expression levels that were detectable by either endpoint PCR or qRT-PCR, whereas the remaining gene was not detected (Table 1). The six expressed genes were characterized, and only RiArsB and RiMT-11 were responsive to As.

#### 3.2. The arsenate/arsenite permease (RiArsB) protein

RiArsB belongs to the ArsB–NhaD-permease superfamily, although it only shares 26 % identity with a hypothetical *Spizellomyces punctatus* protein (XP\_016611517.1). Nevertheless, RiArsB

**Table 1**

Primers used to investigate the role of *G. intraradices* genes in As transport or detoxification.

Gene name	Protein ID	Forward primer	Reverse primer	Length (bp)	cDNA position
ArsA ABC ATPase <sup>b</sup>	342665	CGCAATTAAGTGGACGGTIT	CGITCAATCCCATCATACCC	171	1006–1176
ArsB arsenate/arsenite permease	211650	AACCCACAAAAGCCACAAC	GTCAATATGGCGTCTTCATCGG	143	693–835
ArsC arsenate reductase	340767	CGGTGAAAGAAGGAGATGCAAC	GGCGAGCAATGATAGCTTTACC	144	242–385
Arsenite-resistance protein 2	215498	CCTTAGAGGCGTGCTAGGTG	CTTCGACGACGTGTTCTTGA	209	648–846
Methyltransferase type 11	349203	GCAAAAGATTCCATCCCAGA	TACCCTCTGGACCAACCAAC	187	414–600
Phytochelatin synthase	46746	CAGGGCCGTAATACCTGA	CGGAGCACCTGTGACTTGTGA	201	7–207
Tyrosine phosphatase/arsenate reductase-1 <sup>a</sup>	345591	CGGGTACTGCAGGTTTCAT	GATTGCTTTTGATCCCTTCG	200	149–348

Protein ID refers to the number assigned in the transcriptome project database.

<sup>a</sup> Indicates no expression was detected in cDNA obtained from *R. irregularis* external hyphae added with As for 4 h by end point RT-PCR or qRT-PCR.

<sup>b</sup> Indicates that the gene was previously described as responsive to arsenate addition (González-Chávez et al., 2011).

shows conserved features with other members of this permease superfamily, which are predicted to contain 8–13 transmembrane helices. The Protter-supported transmembrane topology of *RiArsB* predicts ten transmembrane helix domains and that the protein's N- and C-termini are extracellular (Fig. S1). The predicted localization of *ArsB* was the plasma membrane (prediction confidence 21). The *RiArsB* protein has 573 amino acid residues, a MW of 64.4176 kDa and an isoelectric point of 5.6, with an estimated half-life in yeast >20 h. Putative motifs include five putative ASN-glycosylation domains (Fig. S1), while other conserved domains include ten myristylation sites, and two cAMP-, five PKC-, two TYR- and nine CK2-phosphorylation sites.

### 3.3. The methyltransferase type 11 (*RiMT-11*) protein

The *RiMT-11* amino acid sequence shows homology to members of the S-adenosylmethionine-dependent methyltransferase superfamily (SAM or AdoMet-MTase), class I. *RiMT-11* has 361 amino acid residues, a predicted molecular weight of 40.3079 kDa, an isoelectric point of 5.63, and an estimated half-life in yeast >20 h. The predicted localization of *RiMT-11* was the cytoplasm (prediction confidence 30). Motifs included three putative ASN-glycosylation sites, four myristylation sites, and nine PKC- and ten CK2- phosphorylation sites. The VLDLGSMSG motif (residues 90–98), which is associated with the binding of AdoMet by the enzyme, was determined to closely match the (V/I/L)(L/V)(D/E)(V/I)G(G/C)G(T/P)G consensus sequence.

### 3.4. *RiMT-11* and *RiArsB* expression is induced in response to arsenate

*RiMT-11* and *RiArsB* were both responsive to the addition of 350  $\mu$ M arsenate to liquid medium in two-compartment plates (Figs. 1 and 2, respectively). Induction of gene expression in most cases was detected 1 h after arsenate addition. A significantly higher expression was observed at 4 h than at 24 h for both genes. Thus, experiments conducted in the three independent experimental units demonstrated the same pattern of transcript accumulation for both genes (Insets in Figs. 1 and 2). In addition, a short time course experiment was conducted with 350  $\mu$ M arsenate over 12 h, in order to investigate the relative gene expression in *RiMT-11*

and *RiArsB*. This experiment showed maximum induction peaks at times ranging from 4 to 6 h (Fig. 3). Furthermore, when the experiment was performed with three independent plates, induction peaks were detected at 4 or 6 h after As addition, with variable results depending on each experimental unit (data not shown). Based on these results, we interpreted the 4 h time point as a period when induction of these two genes is always present, even though it did not represent the peak (as observed with *RiArsB*). Consequently, this 4-h time point was selected for measurements in further experiments.

Next, we performed a dose–response experiment with arsenate concentrations ranging from 0 to 3500  $\mu$ M, revealing that 350  $\mu$ M arsenate after 4 h induced the highest expression levels in both *RiMT-11* and *GiPT*. The highest expression levels in *RiArsB* were induced by 3500  $\mu$ M arsenate, although the differences were not statistically significant (Fig. 4).

The relative expression of other expressed genes was quantified in both, the time course and the dose response experiments (data not shown), including *ArsC* arsenate reductase, arsenite-resistance protein 2, and phytochelatin synthase (Table 1). However, no changes in their transcript levels were detected (data not shown). Since the earliest time point in our time course experiment was 1 h after addition of As(V), we conducted additional experiments in which we sampled 10 and 30 min after the addition of As(V); however we were not able to detect any change in *RiArsC* transcripts levels (data not shown). *RiArsC* was expressed constitutively, its relative expression levels were similar to non-induced *GiPT* or *GiArsA* (data not shown). *RiArsC* protein shares low identity (30–36 %) to different hypothetical proteins of fungal origin with non-described functions, and to arsenate reductases from bacterial origin.

### 3.5. *RiMT-11* and *RiArsB* expression is not induced by phosphate

*GiPT* and *GiArsA* are reported to be inducible at a phosphate medium concentration of 35  $\mu$ M (González-Chávez et al., 2011), which is the same low phosphate concentration present in M medium. *RiMT-11* and *RiArsB* transcripts did not accumulate in response to the addition of low (35  $\mu$ M) phosphate at 4 h as compared to time zero (Fig. 5), whereas *GiPT* and *GiArsA* displayed induced transcript levels at 4 h. *RiMT-11* did not respond to

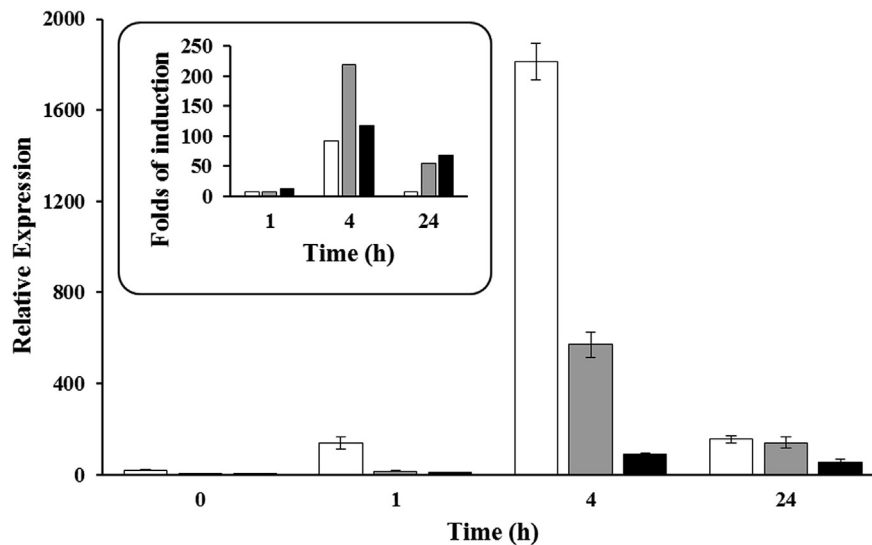


**Fig. 1.** Time course of *RiMT-11* gene expression in response to the addition of arsenate (350  $\mu$ M). Each color bar represents a different two-compartment system. Each bar represents the measurement of two sample replicates (mycelium pieces), each one measured in triplicate per plate. Bars represent the mean value and error bars indicate the standard deviation. The inset figure shows fold of induction relative to zero time, calculations were made based on the mean value of relative expression.

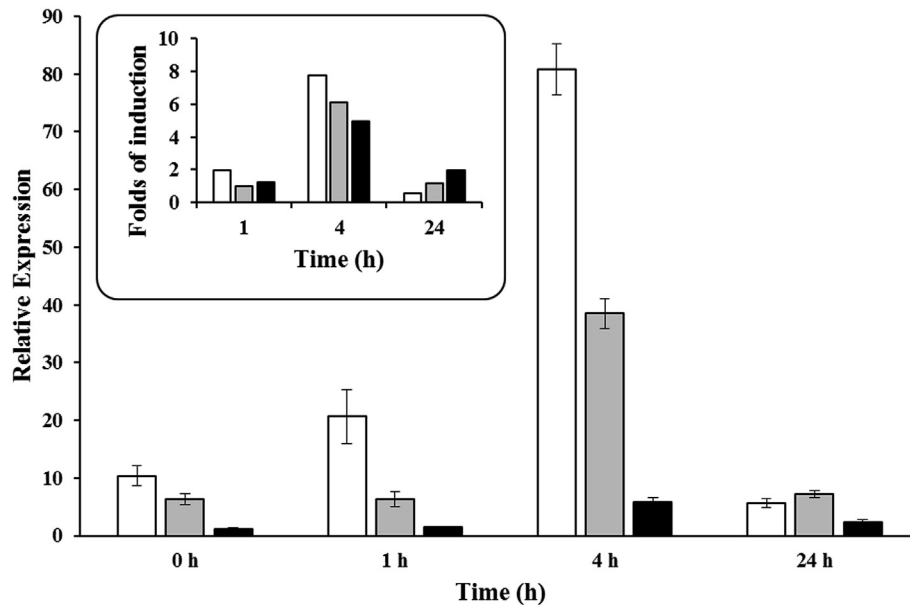


**Fig. 2.** Time course of *RiArsB* gene expression in response to the addition of arsenate (350 μM). Each color bar represents a different two-compartment system. Each bar represents the measurement of two sample replicates (mycelium pieces), each one measured in triplicate. Bars represent the mean value and error bars indicate the standard deviation. The inset figure shows fold of induction relative to zero time, calculations were made based on the mean value of relative expression.

phosphate addition, although it did respond to 350 μM arsenate at both 4 h and 24 h (Fig. 6).

### 3.6. *RiMT-11* and *RiArsB* gene expression is induced in the root compartment

End-point PCR revealed that both *RiArsB* and *RiMT-11* are expressed in *M. truncatula* root tissues colonized with *R. irregularis*

for 7 weeks (~70 % colonization efficiency; Fig. S2). Two-compartment systems with depleted phosphate were subsequently used to examine whether the relative gene expression in *RiArsB* and *RiMT-11* is also induced in response to arsenate addition, in root tissues from the ‘plant + fungus’ compartment.

Carrot hairy root tissues colonized with *R. irregularis* (~70 % colonization efficiency) from the plant side of a two-compartment system displayed an accumulation in *RiArsB* and *RiMT-11* transcript levels in response to arsenate addition (Fig. 7). The *GiPT* control was measured and observed to follow a trend similar to *RiArsB* and *RiMT-11*.

Transcript levels for *GiPT* showed similar expression levels in both the intra-radical mycelium (IRM), and the extra-radical mycelium (ERM), and showed similar folds of induction at 4 h after As(V) addition in both locations (Table S1). *RiArsB* and *RiMT-11* showed higher expression levels in ERM than in IRM. However, folds of induction at 4 h after As(V) addition were higher in the IRM than in the ERM (Table S1).

### 3.7. *RiMT-11* transcript accumulation in response to arsenate is independent of phosphate loading in arbuscular mycorrhiza

*M. truncatula* R108 (wild type) and *mtpt4/mtpt8* double mutant plants (Breuillin-Sessoms et al., 2015) colonized with *R. irregularis* were used to investigate the possible role of *RiArsB* and *RiMT-11* in arsenate detoxification, independently of symbiotic P transport. Ten-week old *R. irregularis* colonized root tissues of P-starved *M. truncatula* *mtpt4/mtpt8* double mutant plants and R108 wild type plants maintained in a semi-sterile system where roots were kept sterile were used. We observed an accumulation in *RiMT-11* and *RiArsB* transcripts in response to As addition in the phosphate-starved double mutant and wild type plants. *RiMT-11* transcripts accumulated at both 4 h and 24 h, whereas *RiArsB* transcripts accumulated only at 24 h (Fig. 8A and B), as observed in external hyphae (Figs. 1 and 3) or roots colonized with hyphae (Fig. 7). No accumulation was observed in *GiPT* transcript levels with the exception of the double mutant, which exhibited a significant but slight increase (approximately 2-fold) at 24 h with respect to the wild type after arsenic addition (Fig. 8C).

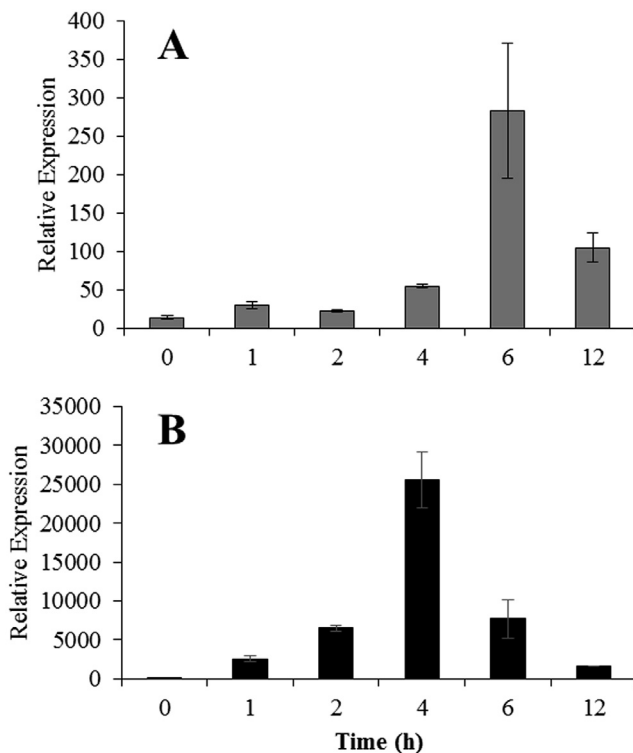


**Fig. 3.** Time course experiment showing the pattern of transcript accumulation at 350 μM arsenate for (A) *RiArsB* and (B) *RiMT-11*.

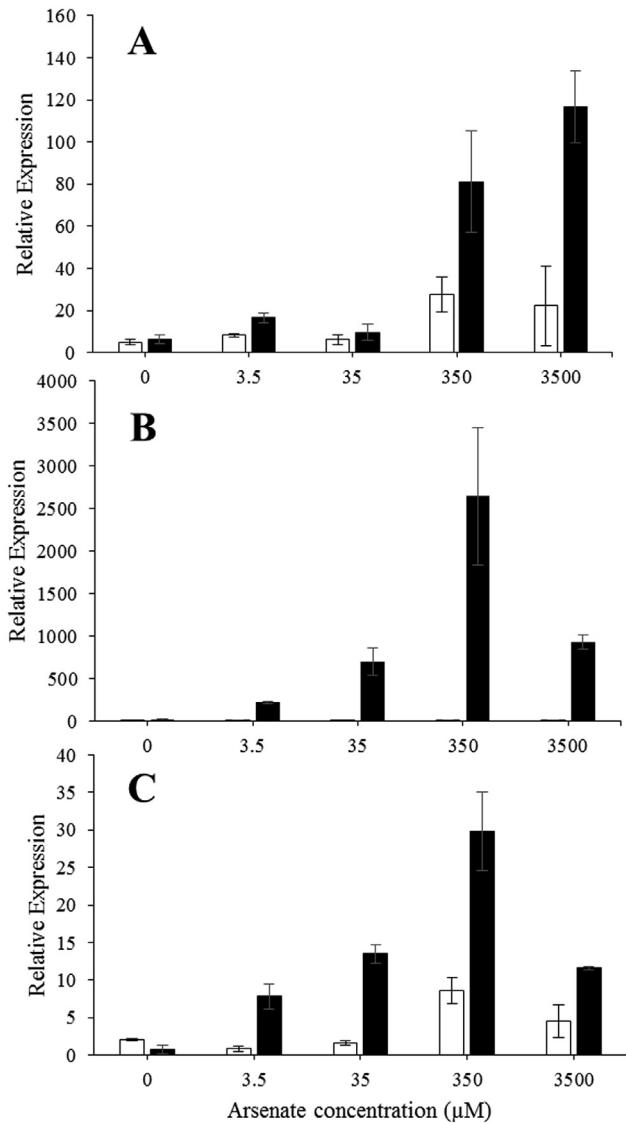


**Fig. 4.** Dose–response experiment showing the induction pattern of (A) *RiArsB*, (B) *RiMT-11* and (C) the *GiPT* control. Open bars correspond to controls measured at 0 h in the same experimental unit, whereas closed bars are samples treated with arsenate for 4 h.

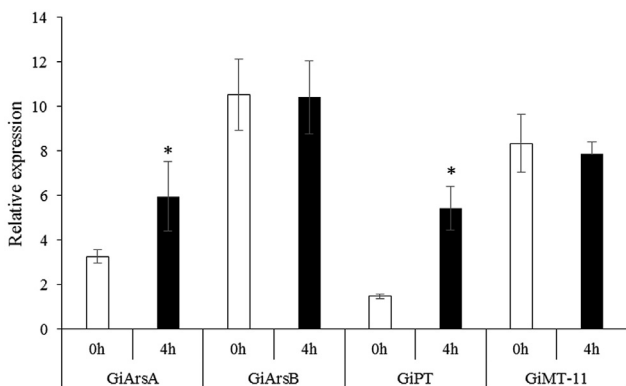


**Fig. 5.** Effect of phosphate addition (35 μM) on gene expression at time zero (open bars) and after 4 h (closed bars). Plates used for the experiment contained >0.15 μM of residual phosphate in the liquid medium at time zero. Asterisks indicate differences between 0 h and 4 h treatment (Student's t-test,  $p > 0.01$ ).

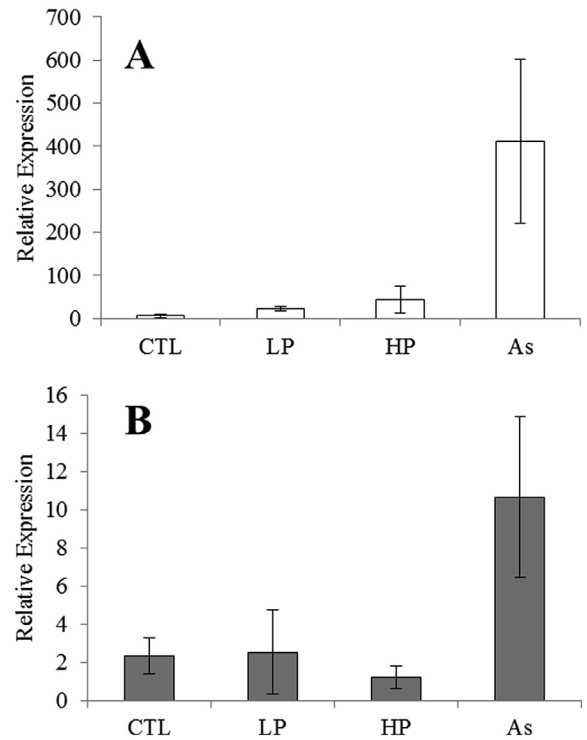


**Fig. 6.** Effect of phosphate and arsenate addition on the expression of *RiMT-11* at (A) 4 h and (B) 24 h. LP: low phosphate, 35 μM; HP: high phosphate, 350 μM; As: 350 μM As. Plates used for the experiment contained >0.15 μM of residual phosphate in the liquid medium at time zero.

## 4. Discussion

### 4.1. Expression of putative arsenic-related genes

Data mining of the *R. irregularis* genome (Tisserant et al., 2013) and transcriptome (Tisserant et al., 2012; Lin et al., 2014) identified seven genes predicted to be involved in As transport and detoxification. The expression of six of these genes was detected by PCR or qRT-PCR. For the seventh gene, our inability to detect transcripts might be due to very low expression levels observed under the particular conditions of these experiments. The main goal of this work was to find novel genes responsive to As addition, but we do not exclude the possibility that these genes could be induced by other metalloids.

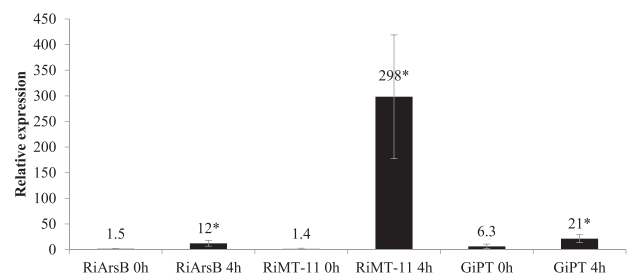


**Fig. 7.** Induction of *RiArsB*, *RiMT-11* and *GiPT* transcript levels in root tissue containing intraradical hyphae, 4 h after the addition of arsenate (350 μM). Plates used for the experiment contained >0.15 μM of residual phosphate in the liquid medium at time zero. Numbers are provided to indicate the relative expression values for each bar. Asterisks indicate a statistically significant change related to the control at 0 h (Student's t-test,  $p > 0.05$ ).

#### 4.2. The *RiArsB* and *RiMT-11* proteins

*ArsB*–NhaD permeases (cl28396) translocate different organic and inorganic (e.g. arsenite and antimonite) anions across biological membranes. *RiArsB* was predicted to be a membrane protein containing ten transmembrane helix domains (Fig. S1) that may function independently as a chemiosmotic transporter ( $\text{Na}^+/\text{H}^+$  antiporter), or as a channel-forming subunit coupled to an ATP-driven anion pump (*ArsAB*) for arsenite efflux in *R. irregularis*, as reported in bacteria (Dey and Rosen, 1995).

A putative *GiArsA* ABC ATPase gene has already been described in *R. irregularis* (previously known as *G. intraradices*) (González-Chávez et al., 2011) which is responsive to As addition. First, the transcript levels of *GiPT*, a putative high-affinity phosphate transporter that could introduce arsenate to the fungal mycelium, are induced. Second, transcripts of *GiArsA*, a putative component of the *R. irregularis* arsenite efflux pump, are induced. This is in agreement with a proposed As exclusion mechanism that involves the

reduction of As(V) to As(III) species, followed by efflux to the external mycelium (González-Chávez et al., 2011). As(V) uptake, reduction to As(III), and efflux of the As species have been demonstrated in the external hyphae of *R. irregularis* (González-Chávez et al., 2014). Thus, it is possible that *RiArsB* may be the permease portion of a putative *ArsAB* arsenite efflux pump, in which it interacts with *GiArsA* to allow arsenite efflux to the exterior of the AMF mycelium. Nevertheless, this hypothesis requires further exploration at this time.

*RiMT-11* is predicted to be a cytoplasmic class I AdoMet-MTase. The enzymes within this class can exhibit different substrate specificities and different target atoms for methylation, including arsenite (Lin et al., 2002). The discovery of *RiMT-11* in *R. irregularis* also provides new evidence for possible detoxification mechanisms involving As methylation in AMF, as discussed below.

#### 4.3. *RiArsB* and *RiMT-11* expression is induced in response to arsenate

Both *RiArsB* and *RiMT-11* displayed a rapid induction response to the addition of exogenous arsenate (350  $\mu\text{M}$ ). *RiMT-11* and *GiPT* transcripts reached their highest accumulation at 350  $\mu\text{M}$ , whereas *RiArsB* transcripts continued increasing up to 3500  $\mu\text{M}$  arsenate. *GiPT* was selected as a control in this study due to its previous characterization in the two-compartment system (Maldonado-Mendoza et al., 2001; González-Chávez et al., 2011). *GiPT* is a high-affinity phosphate transporter whose transcript levels accumulate in response to the addition of low phosphate (35  $\mu\text{M}$ ) in the external medium surrounding the fungal hyphae, but not in response to high phosphate (3500  $\mu\text{M}$ ) (Maldonado-Mendoza et al., 2001). The expression of this gene has been characterized in response to As(V) addition, demonstrating that high levels of arsenate induce its expression at 350 and 3500  $\mu\text{M}$  (González-Chávez et al., 2011), consistent with our results.

#### 4.4. Phosphate does not induce relative gene expression in *RiArsB* or *RiMT-11*

The low-level addition of phosphate (35  $\mu\text{M}$ ) did not alter transcript levels of either *RiArsB* or *RiMT-11* (Fig. 5). In this experiment, *GiPT* and *GiArsA* were included as controls to demonstrate the effect of phosphate addition on their expression. These two genes exhibit an increase in transcript accumulation when exposed to low phosphate addition (González-Chávez et al., 2011), similar to our results in the present study (Fig. 5). In addition, *RiMT-11* was not responsive to high phosphate addition (350  $\mu\text{M}$ ), indicating that its expression is specifically regulated by arsenate addition (Fig. 6).

#### 4.5. *RiArsB* and *RiMT-11* gene expression was induced in the root compartment and is independent of phosphate loading in arbuscular mycorrhiza

*RiArsB* and *RiMT-11* were expressed in *R. irregularis*-colonized *M. truncatula* root tissues that had not received arsenate (Fig. S2). Expression of *GiPT* and *GiArsA* in intraradical hyphae has been demonstrated using cortex cells containing arbuscules dissected by laser ablation (González-Chávez et al., 2011). When colonized transformed carrot root tissue was manipulated in the two-compartment plate system to measure transcript levels of both genes, we found both: basal levels of expression and a similar transcript induction response to the addition of arsenate (Fig. 7) as observed in the external fungal mycelium. In fact, the induction of *RiArsB* and *RiMT-11* in IRM was higher than in the ERM, although basal (0 h) and induced (4 h after As addition) levels of expression were about one order of magnitude higher in ERM rather than in

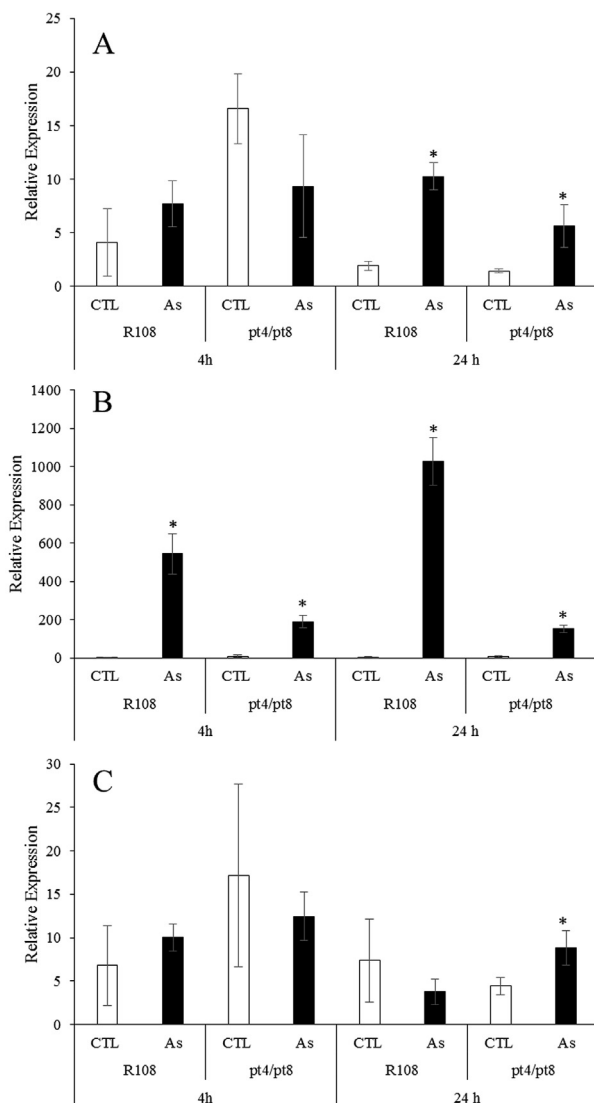


**Fig. 8.** Effect of arsenate addition on *M. truncatula* double mutants in AM-responsive phosphate transporters (*mtp4/mtp8*). (A) *RiArsB*; (B) *RiMT-11*; (C) *GiPT*. The open bars represent control plants and the closed bars represent plants receiving arsenate at the indicated time. R108 refers to wild type plants, while *pt4/pt8* refers to *mtp4/mtp8* double mutants. Asterisks indicate a statistically significant change related to the control at 0 h (Student's t-test,  $p > 0.05$ ).

IRM. The tissue analyzed from *M. truncatula* or transformed carrot roots contained a mix of both internal and external *Rhizophagus intraradices* mycelia. Although the induction response in ERM could suggest that these genes were preferentially expressed in external hyphae, localization studies are needed to demonstrate if they are truly being expressed in the intraradical hyphae.

Although there are 13 Pi transporter genes in *M. truncatula*, *MtPT4* and *MtPT8* are the only two phosphate transporters that are induced during AM colonization, and both genes are expressed within arbuscule-containing cortex cells. *MtPT4* mutations result in premature arbuscule degeneration (PAD); since the fungus fails to establish itself within the roots, the symbiosis is abolished (Javot et al., 2007). A similar phenotype is observed in *mtpt4/mtpt8* double mutants when they are grown in high N conditions, although they exhibit a wild type phenotype under low N (Breuillin-Sessoms et al., 2015), as found in our study. Transcripts of both *RiArsB* and *RiMT-11* increased in response to As addition in the R108 wild type background, as well as in *mtpt4/mtpt8* double mutants (Fig. 8A and B). This suggests that the absence of phosphate loading from the AMF to the plant does not alter the response of these genes to arsenate addition. The lack of response in wild type plants and a slight 2-fold increase in *GiPT* expression in the *mtpt4/mtpt8* double mutant at 24 h (Fig. 8C) may suggest a different temporal response for this gene to arsenic addition under this particular system.

As(V), the main As species in the aerobic environment, functions similar to phosphate and is a competitor for plant phosphate transporters (Asher and Reay, 1979). AMF play key roles in plant acquisition of phosphorus (P) (Smith et al., 2003), which highlights the need to take P–As interactions into account in order to understand the role of AMF in plant uptake of As(V).

Christophersen et al. (2012) reported an increase in arsenic tolerance in *M. truncatula* plants colonized with *Glomus mosseae* vs. *G. intraradices*. Specifically, *G. mosseae* colonized plants showed a higher selectivity against As (P/As molar ratios) and lower expression of the root epidermal phosphate transporter *MtPht1;1* (and to a lesser extent *MtPht1;2*) as compared to *G. intraradices* inoculated plants, suggesting subtle differences between different AMF–plant interactions. In contrast to our proposed model for exclusion of arsenic by AMF, Christophersen et al. (2012) did not find any decrease in specific As uptake at low or high phosphate supplementation in AM plants. This suggests that the increases in specific As uptake in *G. intraradices*-inoculated plants may have been the result of As uptake and delivery via the AM pathway, which is consistent with a high expression level of the arbuscule-associated *M. truncatula* phosphate transporter *MtPht1;4* (Javot et al., 2007).

To date, the protective mechanisms employed by AMF to reduce the toxic effects of arsenic on host plants have been poorly explored. This research has led us to propose an exclusion mechanism for As in AMF. Our previous research has used microspectroscopic X-ray fluorescence ( $\mu$ -XRF) and microspectroscopic X-ray absorption near edge structure ( $\mu$ -XANES) analyses to decipher AMF As-speciation mechanisms, revealing that once As(V) enters the fungal hypha it is rapidly reduced to As(III), possibly via an arsenate reductase (González-Chávez et al., 2014). Although our data mining in the present study identified a putative arsenate reductase with detectable expression, we did not observe any transcript changes in this gene in response to As addition (data not shown). The reduction of As(V) to As(III) requires 0–1 h following As(V) exposure in *R. irregularis* extraradical hyphae exposed to As (González-Chávez et al., 2014). At 1–6 h, arsenic is found as different compounds, in which the most dominant species is an As(III)–Fe(II) carbonate form, along with less abundant forms such as As(V)–Fe(III) hydroxide and As(III)–sulfur compounds. After 24 h exposure, As becomes undetectable in the external hyphae. This is possibly mediated by a putative *ArsAB* arsenite efflux pump.

The ABC ATPase component (*GiArsA*) is induced after 3 h of As addition (González-Chávez et al., 2011), and here we have described a putative *RiArsB* permease component of the efflux pump that is induced as soon as 1–4 h after As addition (Figs. 2 and 3). Their patterns of gene expression suggest that the two putative components of the arsenite efflux pump are located in both internal and external hyphae, which may be required for their interaction. Further research is required to confirm whether such an interaction between *GiArsA* and *RiArsB* occurs and both are part of the *R. irregularis* arsenite efflux pump. Further work is also needed to confirm the involvement of an arsenate reductase needed for the fast reduction from As(V) to As(III) reported in *R. irregularis* extraradical mycelium (González-Chávez et al., 2014). No evidence for transcript accumulation of the putative arsenate reductase *RiArsC* gene in response to As(V) addition was detected in this work. Demonstrating protein function for *GiArsA*, *RiArsB* and *RiArsC* is needed in order to understand the roles that these genes may play in *R. intraradices* and As(V) addition. Although we attempted to complement yeast mutants defective on these three genes our efforts were not successful (data not shown).

In support of our proposed As(III) exclusion mechanism in AMF, recent research has shown that treating maize with P and AMF moderately increases As(III) in the rhizosphere, with As(III) concentrations in soil layers surrounding roots decreasing towards the bulk soil (Cattani et al., 2015). It is also possible that As(III) is rapidly transported to the plant, consistent with the observations of Zhang et al. (2015b), who described an increase of As(III) in *M. truncatula* mycorrhiza. However, this is not in agreement with our observations made in two-compartment plates with carrot transformed roots, where we were unable to detect As in the roots following As addition to the 'plant + fungus' compartment employing  $\mu$ -XRF and  $\mu$ -XANES analyses (González-Chávez et al., 2014). Nonetheless, it is possible in our previous study that As was present at undetectable levels in the carrot roots.

Our identification of the As-responsive methyltransferase *RiMT-11* is an important finding in this work, since it provides novel evidence for a possible As methylation mechanism mediated by AMF. Recently, DMA accumulation was reported in the shoots of *M. truncatula* exclusively in mycorrhizal plants (Zhang et al., 2015b). This supports the idea that *RiMT-11* may produce the DMA that is transferred to the plant. Nevertheless, these findings are inconsistent with a previous study (González-Chávez et al., 2014) that was unable to detect monomethylarsinic acid (MMA) or DMA in the external hyphae of *R. irregularis*. In bacteria such as *Rhodopseudomonas palustris* (Qin et al., 2006) or *Pseudomonas alcaligenes* (Zhang et al., 2015a), S-adenosylmethionine (AdoMet) methyltransferase confers As(III) resistance by catalyzing the formation of a number of methylated intermediates from As(III), including DMA, with the production of trimethylarsine [TMA(III)] gas as an end product. This gaseous methylated form results in the loss of arsenic from the medium and the cells, and confers a mechanism for As tolerance to these bacteria. The possibility of a similar mechanism in AMF could explain the absence of detectable MMA or DMA in AMF. *RiMT-11* must be characterized and its enzymatic capabilities analyzed in order to further investigate the possible detoxification mechanisms mediated by AMF As methylation. Future research should incorporate radioactive As tracer experiments or  $\mu$ -XRF and  $\mu$ -XANES analyses in order to understand As transport in arbuscular mycorrhiza, and the fate of As from AMF to the host plants.

## 5. Conclusions

Our results provide novel information on two undescribed genes that respond to exogenous As(V) addition in AMF: *RiArsB* and *RiMT-11*. *RiArsB* is suggested to be involved in As(III) exclusion by

pumping As(III) out of the fungus, whereas RiMT-11 may have a role in the methylation of arsenic as a putative detoxification mechanism in AMF. These results require further biochemical and physiological characterization to provide a clear understanding of the mechanisms that AMF utilize to increase arsenic tolerance in plants.

## Acknowledgments

IEMM received a one year sabbatical fellowship from the National Council for Science and Technology (CONACyT) of Mexico (Proposal No. 246225) and from the Instituto Politécnico Nacional (IPN) of Mexico (2014-720-1-63). This work was partially supported by the Instituto Politécnico Nacional of Mexico, grants SIP 20144103 and SIP 20150775 and the Agriculture and Food Research Initiative competitive grant no. 2014-67013-21571 of the U.S. Dept. of Agriculture, National Institute of Food and Agriculture. The authors would like to thank Veronique Levesque-Tremblay and Dierdra A. Daniels for their technical help.

## Appendix A. Supplementary data

Supplementary data related to this article can be found at <https://doi.org/10.1016/j.funbio.2017.11.003>.

## References

- Ames, B.N., 1966. Assay of inorganic phosphate, total phosphate and phosphatases. In: Neufeld, E., Ginsburg, V. (Eds.), *Methods in Enzymology*, Complex Carbohydrates, vol. 8. Academic Press, New York, pp. 115–118.
- Asher, D.J., Reay, P.F., 1979. Arsenic uptake by barley seedlings. *Aust. J. Plant Physiol.* 6, 459–466.
- Bai, J.F., Lin, X.G., Yin, R., Zhang, H.Y., Wang, J.H., Chen, X.M., Luo, Y.M., 2008. The influence of arbuscular mycorrhizal fungi on As and P uptake by maize (*Zea mays* L.) from As-contaminated soils. *Appl. Soil Ecol.* 38, 137–145.
- Bécard, G., Fortin, J.A., 1988. Early events of vesicular-arbuscular mycorrhiza formation on Ri T-DNA transformed roots. *New Phytol.* 108, 211–218.
- Breuillan-Sessoms, F., Floss, D.S., Gomez, S.K., Pumplin, N., Ding, Y., Levesque-Tremblay, V., Noar, R.D., Daniels, D.A., Bravo, A., Eaglesham, J.B., Benedito, V.A., Udvardi, M.K., Harrison, M.J., 2015. Suppression of arbuscule degeneration in *Medicago truncatula phosphate transporter4* mutants is dependent on the ammonium transporter 2 family protein AMT2;3. *Plant Cell* 27, 1352–1366.
- Cattani, I., Beone, G.M., Gonnelli, C., 2015. Influence of *Rhizoglyphus irregularis* inoculation and phosphorus application on growth and arsenic accumulation in maize (*Zea mays* L.) cultivated on an arsenic-contaminated soil. *Environ. Sci. Pollut. Res.* 22, 6570–6577.
- Cervantes-Gómez, R.G., Bueno-Ibarra, M.A., Cruz-Mendivil, C.L., Calderón Vázquez, C.L., Ramírez-Douriet, C.M., Maldonado-Mendoza, I.E., Villalobos-López, M.A., Valdez-Ortiz, A., López-Meyer, M., 2015. Arbuscular mycorrhizal symbiosis-induced expression changes in *Solanum lycopersicum* leaves revealed by RNA-seq analysis. *Plant Mol. Biol. Rep.* 34, 89.
- Chen, B.D., Xiao, X.Y., Zhu, Y.G., Smith, F.A., Xie, Z.M., Smith, S.E., 2007. The arbuscular mycorrhizal fungus *Glomus mosseae* gives contradictory effects on phosphorus and arsenic acquisition by *Medicago sativa* Linn. *Sci. Total Environ.* 379, 226–234.
- Chen, X., Li, H., Chan, W.F., Wu, C., Wu, F., Wu, S., Wong, M.H., 2012. Arsenite transporters expression in rice (*Oryza sativa* L.) associated with arbuscular mycorrhizal fungi (AMF) colonization under different levels of arsenite stress. *Chemosphere* 89, 1248–1254.
- Christophersen, H.M., Smith, F.A., Smith, S.E., 2009. Arbuscular mycorrhizal colonization reduces arsenate uptake in barley via downregulation of transporters in the direct epidermal phosphate uptake pathway. *New Phytol.* 184, 962–974.
- Christophersen, H.M., Smith, F.A., Smith, S.E., 2012. Unraveling the influence of arbuscular mycorrhizal colonization on arsenic tolerance in *Medicago: Glomus mosseae* is more effective than *G. intraradices*, associated with lower expression of root epidermal Pi transporter genes. *Front. Physiol.* 3, 91.
- Dey, S., Rosen, B.P., 1995. Dual mode of energy coupling by the oxyanion-translocating ArsB protein. *J. Bacteriol.* 177, 385–389.
- Doner, L.W., Bécard, G., 1991. Solubilization of gellan gels by chelation of cations. *Biotechnol. Tech.* 5, 25–28.
- Dong, Y., Zhu, Y.G., Smith, F.A., Wang, Y., Chen, B.D., 2008. Arbuscular mycorrhiza enhanced arsenic resistance of both white clover (*Trifolium repens* Linn.) and ryegrass (*Lolium perenne* L.) plants in an arsenic-contaminated soil. *Environ. Pollut.* 155, 174–181.
- Floss, D.S., Schmitz, A.M., Starker, C.G., Gantt, J.S., Harrison, M.J., 2013. Gene silencing in *Medicago truncatula* roots using RNAi. In: Rose, R.J. (Ed.), *Methods in Molecular Biology*, Legume Genomics: Methods and Protocols, vol. 1064. Humana Press, New Delhi, pp. 163–177.
- Garg, N., Singla, P., 2012. The role of *Glomus mosseae* on key physiological and biochemical parameters of pea plants grown in arsenic contaminated soil. *Sci. Hortic.* 143, 92–101.
- González-Chávez, C., Harris, P.J., Dodd, J., Meharg, A.A., 2002. Arbuscular mycorrhizal fungi confer enhanced arsenate resistance on *Holcus lanatus*. *New Phytol.* 155, 163–171.
- González-Chávez, MdCA., Ortega-Larrocea, MdP., Carrillo-González, R., López-Meyer, M., Xoconostle-Cázares, B., Gomez, S.K., Harrison, M.J., Figueroa-López, A.M., Maldonado-Mendoza, I.E., 2011. Arsenate induces the expression of fungal genes involved in As transport in arbuscular mycorrhiza. *Fungal Biol.* 115, 1197–1209.
- González-Chávez, MdCA., Miller, B., Maldonado-Mendoza, I.E., Scheckel, K., Carrillo-González, R., 2014. Localization and speciation of arsenic in *Glomus intraradices* by synchrotron radiation spectroscopic analysis. *Fungal Biol.* 118, 444–452.
- Hildebrandt, U., Regvar, M., Bothe, H., 2007. Arbuscular mycorrhiza and heavy metal tolerance. *Phytochemistry* 68, 139–146.
- Javot, H., Penmetsa, R.V., Terzaghi, N., Cook, D.R., Harrison, M.J., 2007. A *Medicago truncatula* phosphate transporter indispensable for the arbuscular mycorrhizal symbiosis. *Proc. Natl. Acad. Sci. U. S. A.* 104, 1720–1725.
- Jia, Y., Huang, H., Sun, G.X., Zhao, F.J., Zhu, Y.G., 2012. Pathways and relative contributions to arsenic volatilization from rice plants and paddy soil. *Environ. Sci. Technol.* 46, 8090–8096.
- Lanfranco, L., Young, J.P.W., 2012. Genetic and genomic glimpses of the elusive arbuscular mycorrhizal fungi. *Curr. Opin. Plant Biol.* 15, 454–461.
- Leung, H.M., Wu, F.Y., Cheung, K.C., Ye, Z.H., Wong, M.H., 2010. Synergistic effects of arbuscular mycorrhizal fungi and phosphate rock on heavy metal uptake and accumulation by an arsenic hyperaccumulator. *J. Hazard. Mater.* 181, 497–507.
- Lin, S., Shi, Q., Nix, F.B., Styblo, M., Beck, M.A., Herbin-Davis, K.M., Hall, L.L., Simeonsson, J.B., Thomas, D.J., 2002. A novel S-adenosyl-L-methionine:arsenic(III) methyltransferase from rat liver cytosol. *J. Biol. Chem.* 277, 10795–10803.
- Lin, K., Limpens, E., Zhang, Z., Ivanov, S., Saunders, D.G.O., Mu, D., Pang, E., Cao, H., Cha, H., Lin, T., Zhou, Q., Shang, Y., Li, Y., Sharma, T., van Velzen, R., de Ruijter, N., Aanen, D.K., Win, J., Kamoun, S., Bisseling, T., Geurts, R., Huang, S., 2014. Single nucleus genome sequencing reveals high similarity among nuclei of an endomycorrhizal fungus. *PLoS Genet.* 10, e1004078.
- Liu, Y., Zhu, Y.G., Chen, B.D., Christie, P., Li, X.L., 2005. Yield and arsenate uptake of arbuscular mycorrhizal tomato colonized by *Glomus mosseae* BEG167 in As spiked soil under glasshouse conditions. *Environ. Int.* 31, 867–873.
- Maldonado-Mendoza, I.E., Dewbre, G.R., Harrison, M.J., 2001. A phosphate transporter gene from the extraradical mycelium of an arbuscular mycorrhizal fungus *Glomus intraradices* is regulated in response to phosphate in the environment. *Mol. Plant Microbe Interact.* 14, 1140–1148.
- McGonigle, T.P., Miller, M.H., Evans, D.G., Fairchild, G.L., Swan, J.A., 1990. A new method which gives an objective measure of colonization of roots by vesicular-arbuscular mycorrhizal fungi. *New Phytol.* 115, 495–501.
- Ortowska, E., Godzik, B., Turnau, K., 2012. Effect of different arbuscular mycorrhizal fungal isolates on growth and arsenic accumulation in *Plantago lanceolata* L. *Environ. Pollut.* 168, 121–130.
- Qin, J., Rosen, B.P., Zhang, Y., Wang, G., Franke, S., Rensing, C., 2006. Arsenic detoxification and evolution of trimethylarsine gas by a microbial arsenite S-adenosylmethionine methyltransferase. *Proc. Natl. Acad. Sci. U. S. A.* 103, 2075–2080.
- Rosen, B.P., Weigel, U., Karkaria, C., Gangola, P., 1988. Molecular characterization of an anion pump. *J. Biol. Chem.* 263, 3067–3070.
- San Francisco, M.J., Tisa, L.S., Rosen, B.P., 1989. Identification of the membrane component of the anion pump encoded by the arsenical resistance operon of R-factor R773. *Mol. Microbiol.* 3, 15–21.
- Smith, S.E., Read, D.J., 2008. *Mycorrhizal Symbiosis*, third ed. Academic Press, Cambridge, UK.
- Smith, S.E., Smith, F.A., 2011. Roles of arbuscular mycorrhizas in plant nutrition and growth: new paradigms from cellular to ecosystem scales. *Annu. Rev. Plant Biol.* 62, 227–250.
- Smith, S.E., Smith, F.A., Jakobsen, I., 2003. Mycorrhizal fungi can dominate phosphate supply to plants irrespective of growth responses. *Plant Physiol.* 133, 16–20.
- Smith, S.E., Christophersen, H.M., Pope, S., Smith, F.A., 2010. Arsenic uptake and toxicity in plants: integrating mycorrhizal influences. *Plant Soil* 327, 1–21.
- St-Arnaud, M.C., Hamel, C., Vimard, B., Caron, M., Fortin, J.A., 1996. Enhanced hyphal growth and spore production of the arbuscular mycorrhizal fungus *Glomus intraradices* in an in vitro system in the absence of host roots. *Mycol. Res.* 100, 328–332.
- Stockinger, H., Walker, C., Schüssler, A., 2009. ‘*Glomus intraradices* DAOM197198’, a model fungus in arbuscular mycorrhiza research, is not *Glomus intraradices*. *New Phytol.* 183, 1176–1187.
- Tisa, L.S., Rosen, B.P., 1990. Molecular characterization of an anion pump. *J. Biol. Chem.* 265, 190–194.
- Tisserant, E., Kohler, A., Dozolme-Seddas, P., Balestrini, R., Benabdellah, K., Colard, A., Croll, D., Da Silva, C., Gomez, S.K., Koul, R., Ferrol, N., Fiorilli, V., Formey, D., Franken, Ph, Helber, N., Hijri, M., Lanfranco, L., Lindquist, E., Liu, Y., Malbreil, M., Morin, E., Poulain, J., Shapiro, H., van Tuinen, D., Waschke, A., Azcón-Aguilar, C., Bécard, G., Bonfante, P., Harrison, M.J., Küster, H., Lammers, P., Paszkowski, U., Requena, N., Rensing, S.A., Roux, C., Sanders, I.R., Shachar-Hill, Y., Tuskan, G., Young, J.P.W., Gianinazzi-Pearson, V., Martin, F., 2012. The transcriptome of the

- arbuscular mycorrhizal fungus *Glomus intraradices* (DAOM 197198) reveals functional tradeoffs in an obligate symbiont. *New Phytol.* 193, 755–769.
- Tisserant, E., Malbreil, M., Kuo, A., Kohler, A., Symeonidi, A., Balestrini, R., Charron, P., Duensing, N., dit Frey, N.F., Gianinazzi-Pearson, V., Gilbert, L.B., Handa, Y., Herr, J.R., Hijri, M., Koul, R., Kawaguchi, M., Krajinski, F., Lammers, P.J., Masclaux, F.G., Murat, C., Morin, E., Ndikumana, S., Pagni, M., Petitpierre, D., Requena, N., Rosikiewicz, P., Riley, R., Saito, K., San Clemente, H., Shapiro, H., van Tuinen, D., Bécard, G., Bonfante, P., Paszkowski, U., Shachar-Hill, Y.Y., Tuskan, G., Young, J.P.W., Sanders, I.R., Henrissat, B., Rensing, S.A., Grigoriev, I.V., Corradi, N., Roux, C., Martin, F., 2013. Genome of an arbuscular mycorrhizal fungus provides insight into the oldest plant symbiosis. *Proc. Natl. Acad. Sci. U. S. A.* 110, 20117–20122.
- Wu, J., Tisa, L.S., Rosen, B.P., 1992. Membrane topology of the ArsB protein, the membrane subunit of an anion-translocating ATPase. *J. Biol. Chem.* 267, 12570–12576.
- Xia, Y.S., Chen, B.D., Christie, P., Smith, F.A., Wang, Y.S., Li, X.L., 2007. Arsenic uptake by arbuscular mycorrhizal maize (*Zea mays* L.) grown in an arsenic-contaminated soil with added phosphorus. *J. Environ. Sci.* 19, 1245–1251.
- Xu, P.L., Christie, P., Liu, Y., Zhang, J., Li, X.L., 2008. The arbuscular mycorrhizal fungus *Glomus mosseae* can enhance arsenic tolerance in *Medicago truncatula* by increasing plant phosphorus status and restricting arsenate uptake. *Environ. Pollut.* 156, 215–220.
- Yu, Y., Zhang, S.Z., Huang, H.L., Luo, L., Wen, B., 2009. Arsenic accumulation and speciation in maize as affected by inoculation with arbuscular mycorrhizal fungus *Glomus mosseae*. *J. Agric. Food Chem.* 57, 3695–3701.
- Zhang, J., Cao, T., Tang, Z., Shen, Q., Rosen, B.P., Zhao, F.-J., 2015a. Arsenic methylation and volatilization by arsenite S-adenosylmethionine methyltransferase in *Pseudomonas alcaligenes* NBRC14159. *Appl. Environ. Microbiol.* 81, 2852–2860.
- Zhang, X., Ren, B.-H., Wu, S.-L., Sun, Y.-Q., Lin, G., Chen, B.-D., 2015b. Arbuscular mycorrhizal symbiosis influences arsenic accumulation and speciation in *Medicago truncatula* L. in arsenic-contaminated soil. *Chemosphere* 119, 224–230.